Vortex- and Wake-Induced Vibrations of Two and Three Cylinders Arranged In-line

Stéphane Étienne, Emmanuel Fontaine, Yves-Marie Scolan

Vortex- and Wake-Induced Vibrations of Two and Three Cylinders Arranged In-line

Stéphane Etienne
Mechanical Engineering Department, École Polytechnique de Montréal
Montréal, Québec, Canada
Emmanuel Fontaine
Amog Consulting
Melbourne, Australia
Yves-Marie Scolan
École Centrale de Marseille
Marseille, France.

ABSTRACT

Vortex-induced vibrations (VIV) and galloping effects are studied for the case of two cylinders in tandem arrangement. Both cylinders are allowed to move in X and Y directions and rigidity is kept the same for both directions. The cross-flow around moving cylinders is computed using a specifically designed numerical method which has been thoroughly verified and validated with manufactured solutions and systematic comparisons between numerical and available experimental results. It consists of a monolithic finite element method for solving fluid-structure problems. After validation results, we present configurations for a center-to-center distance L/D = 4 and reduced velocities ranging from 4 to 16 at a laminar Reynolds number of 200.

KEY WORDS: vortex-induced vibrations; wake-induced vibrations; galloping; circular cylinder; tandem arrangement; XY vibrations.

INTRODUCTION

We study vortex-induced vibrations (VIV), interference and galloping phenomena occurring when two and three circular cylinders arranged in-line are placed in a uniform flow. If VIV for single circular cylinders are well documented, VIV, interference and galloping phenomena studies for arrays of cylinders remain sparse since Bokaian and Geoola (1984) and Zdravkovitch (1985). Recent experiments by Germain *et al.* (2006) showed that wake-induced vibrations occur for reduced velocities far beyond than 10. In Germain *et al.* (2006) peak displacements of the rear cylinder are much larger than one diameter transversely and it is also shown that in-line peak vibration amplitudes may be larger than one diameter. Available numerical studies on XY-oscillating in-line cylinders in cross-flow depict results below reduced velocities of 7 [see Fregonesi *et al.* (2001); Mittal and Kumar (2001, 2004); Potanza *et al.* (2005)].

In Etienne (2008), we presented results till values of 10 of the reduced velocity. To shed light on wake-induced vibrations and reveal some of the features highlighted in the work by Germain *et al.* (2006), much larger reduced velocities shall be studied. In this work the range of studied reduced velocities is extended to values of 16. These configurations are studied with a numerical method based on the finite element method.

We have performed a parametric study with respect to the reduced velocity $U_r = U/fD$, with U the uniform flow velocity, f the natural frequency of cylinders in air $f = (k/m)^{1/2}/(2\pi)$ and D their diameter. k is the rigidity of the spring that supports a unit length cylinder and m is its mass per unit length. The non-dimensional center-to-center distance L/D = 4 is kept constant throughout this study. Values of the reduced velocities U_r are in the range 4 to 16.

Note that the reduced velocity can be expressed as $U_r^* = U/(f_n^* D)$, with f_n^* the natural frequency of cylinders in still water. The relation between the two formulas U_r and U_r^* is such that

$$U_r^* = \sqrt{(m^* + 1)/m^*}\, U_r \qquad (1)$$

with $m^* = m/m_a$ the mass ratio and $m_a = \rho\pi D^2/4$.

A Reynolds number value of 200 has been selected for all computations presented here. This work is handled in a two-dimensional frame of reference. This is justified by the low value of the Reynolds number considered here. At this low value of the Reynolds number the flow is laminar. Also with cylinder vibrations, the correlation length of the flow vortical structures is increased. We assume that under these assumptions the flow remains mainly two-dimensional. All variables are expressed in terms of unit length in the 3rd direction.

We have chosen to enrich the solution map with computations for the case of an array of 3 in-line two-degree of freedom cylinders to highlight wake-induced vibrations phenomena. The motivation to explore the behaviour of 3 in-line two-degree of freedom cylinders in cross-flow stems from the fact that the second cylinder undergoes larger vibrations on a larger reduced velocity range than the front one. This induces impacting wake characteristics that are radically different on the third cylinder than on the second one. Thus, one could expect an amplification of vibrations of the third cylinder compared to the second one on the selected range of reduced velocities (U_r = 4 to 16).

We will roughly describe the numerical method employed herein and present three validation cases close to those of the present study. We will then describe results obtained for two- and three-cylinders arrays arranged in-line.

NUMERICAL DETAILS

All computations are performed with a finite element method. The solver has been specifically designed and developed to treat fluid-structure interactions, may they be of rigid solid type as is the case in this article or of flexible type. To sum up, the solver possesses the following characteristics

- Incompressible velocity-pressure formulation of the Navier-Stokes Equations. The mixed method is used in which the pressure is a Lagrange multiplier.
- 3rd order space accuracy thanks to the use of a P2-P1 Taylor-Hood element.
- Up to 5th order Time accuracy for flow and structure on moving meshes by making use of Implicit Runge-Kutta of order 5. In this study all time simulations have been performed with the 3rd order implicit Runge-Kutta scheme.
- Parallel sparse direct solver PARDISO [Schenk and Gärtner (2004, 2006)].
- Implicit method fully coupling all degrees of freedom (Mesh motion, flow variables and structural/solid variables). This code has been thoroughly validated for unsteady flows on moving grids [Etienne *et al.* (2009)].

Configurations of cylinders for the two and three cylinders cases are depicted on Figure 1-2. All cylinders are allowed to move in both directions of space and have same rigidities. In these figures the rigidities k are expressed in terms of the reduced velocity for clarity. We have $k = mU^2/D^2(2\pi/U_r)^2$. This expression shows that the rigidity, the fluid velocity as well as the diameter can be used to adjust the reduced velocity. Experimentally it is more convenient to vary the fluid velocity. It also makes sense since for real applications this is the surrounding flow that varies whereas the structural characteristics are fixed once and for all at installation in most of the cases. In this study we chose to keep the Reynolds number value and the diameters constant. This allows us to compare the answer for the various reduced velocities for a fixed configuration of the fluid flow. We then adjust the reduced velocity by varying the rigidity of cylinders.

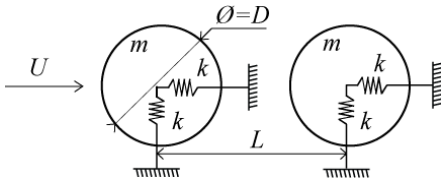

Figure 1: Two cylinders geometry and characteristics.

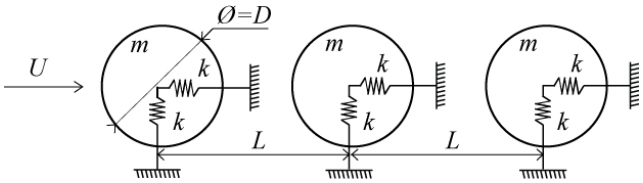

Figure 2: Three cylinders geometry and characteristics.

For the three cylinders cases, center-to-center spacing is the same between the first and second cylinders and second and third cylinders. Figure 3-4 show meshes used for both cases. They are made of 93000 nodes for the tandem case and 118000 nodes for the 3 in-line cylinders arrangement. Distance from first row of nodes to the wall is set to 0.0035*D*. This allows to represent the near-wall boundary layer with the required precision. Also, from Figs. 3-4, one can appreciate the adapted refinement of the mesh that permits to capture the wake characteristics. Non-dimensional simulation time *UT/D* is of 200 and the time step $\Delta t/D = 0.01$. Each case requires approximately 50 hours on a four-node IBM risk machine and 3Go of RAM.

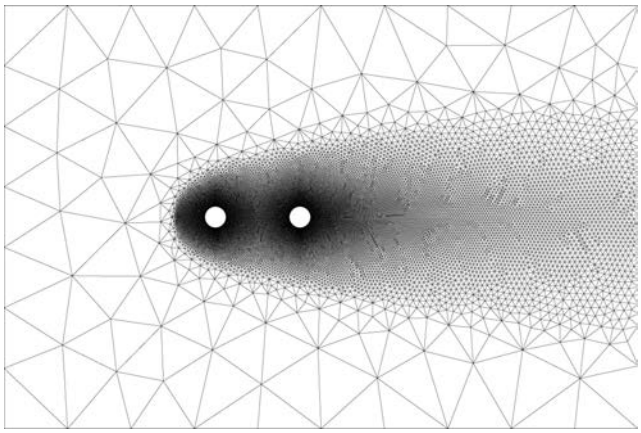
Figure 3: Mesh for the two cylinders case.

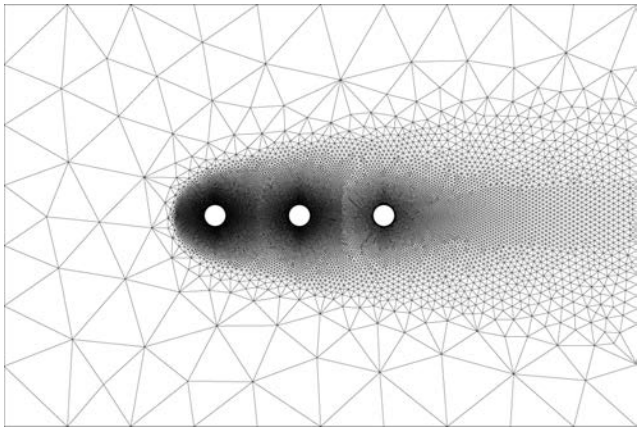
Figure 4: Mesh for the three cylinders case.

VALIDATION

Three validation cases are presented, a fixed circular cylinder in cross-flow at Re = 200, two fixed tandem circular cylinders in cross-flow for various center-to-center spacings at Re = 200 and a single circular cylinder mounted on springs at Re = 200.

For the classical case of a single fixed cylinder in cross flow, we compare on Table 1 results from different references (all numerical references) with those obtained with the present formulation. The drag and lift coefficients and the Strouhal number have been obtained by analysis over a time length of 20 vortex sheddings over which the flow is periodical. The drag coefficient in the mean value of the in-line non-dimensioned force and the lift coefficient is computed as the root mean square of non-dimensioned transverse load. Thus, the transient phase corresponding to the 50 first non-dimensional time units has been discarded. Compared to the other numerical results, those obtained with the present numerical algorithm are in good accordance. However,

while the Strouhal number is well captured, or seems so, lot of scatter can be observed with regards to the lift coefficients among the numerical results collected here. The value we computed is close to the average of the previously computed values, but this is not sufficient to ascertain this is the right lift.

Fixed Single Cylinder	Cd	Cl	St
Halse (1997)	1.35	0.62	0.196
Sa & Chang (1991)	1.13	0.34	0.186
Braza (1981)	1.38	0.76	0.190
Present results	1.36	0.67	0.195

Table 1 : Single fixed cylinder drag, lift and Strouhal number.

The second validation case concerns flows involving two fixed cylinders in tandem arrangement at Re = 200. Center-to-center spacing ratios L/D in the range 1 to 6 have been carried out [see Chagnon 2008)]. The variation of the drag coefficient as a function of center-to-center spacing is shown on Figure 5. We did not find drag coefficients values for flows over tandem cylinders at low Reynolds number values. However Huhe-Aode *et al.* (1985) measured the Strouhal number values for this case at Reynolds numbers of 100 and 300. Table 2 compares Strouhal number values from experiments by Huhe-Aode *et al.* (1985) and our results at Re = 200. It can be observed that numerical values of the Strouhal number compare well with experimental ones. In particular, the increase of the Strouhal number value is similar between experiments and present numerical results. However, in Huhe-Aode *et al.* (1985), the discontinuous change that can be observed on force coefficients on Figure 5 should appear near to L/D = 3.5 at Re = 300 whereas present numerical results predict the discontinuous change at L/D = 3.2±0.015 but for Re = 200. Note also that this discontinuous change decreases with Reynolds number raise and seems to stabilize near to values of L/D = 3 from collected experimental values by Zdravkovitch (1977).

Strouhal number	L/D=3	L/D=5
Re=100 (Huhe-Aode, exp)	0.107	0.141
Re=200 (Present, num)	0.126	0.170
Re=300 (Huhe-Aode, exp)	0.133	0.170

Table 2 : Strouhal number as a function of center-to-center spacing and Reynolds number.

Finally, to validate the whole computational methodology we have chosen a documented case of an isolated cylinder in cross flow. The cylinder is supported by constant springs and dampers in both directions. Its equations of motion in non-dimensional form are

$$\ddot{\mathbf{x}}^* + 2\zeta\left(\frac{2\pi}{U_r}\right)\dot{\mathbf{x}}^* + \left(\frac{2\pi}{U_r}\right)^2 \mathbf{x}^* = \frac{2}{\pi m^*}\begin{bmatrix} C_d \\ C_l \end{bmatrix} \quad (2)$$

$$C_d = \frac{f_x}{\frac{1}{2}\rho D U^2} \quad (3)$$

$$C_l = \frac{f_y}{\frac{1}{2}\rho D U^2} \quad (4)$$

with $\mathbf{x}^* = [x^*, y^*]^T = \mathbf{x}/D$, f_x and f_y the fluid loading for each direction. For this case, we compare with numerical results reported by Blackburn *et al.* (2000) and Yang *et al.* (2008). In both studies as well as in this present validation case the Reynolds number value is equal to 200, the damping ratio ζ is 0.01, the reduced velocity U_r equals 5 and the mass ratio m^* is equal to $4/\pi$.

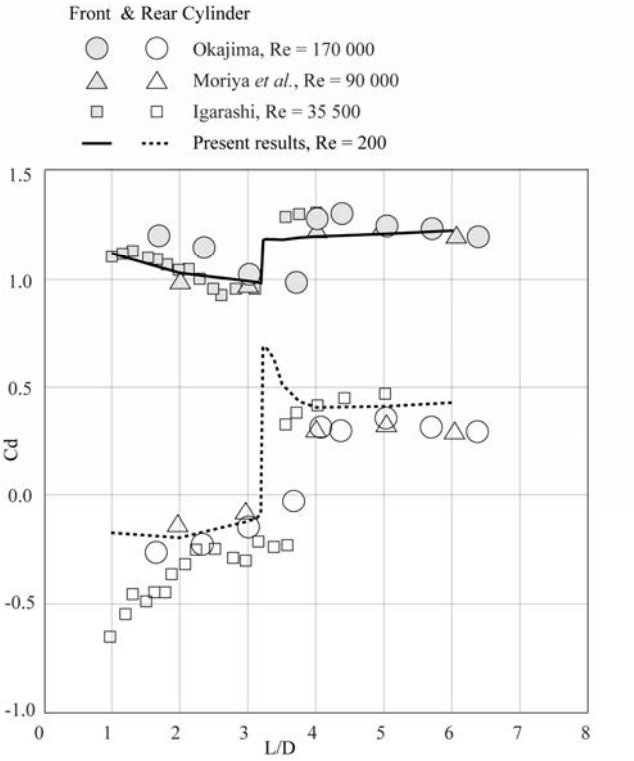

Figure 5 : Drag coefficient for tandem cylinders as a function of center-to-center spacing.

Figure 6 shows the periodical trajectory of the cylinder. Note that on the figure the scale in the horizontal direction extends from 0.6 to 0.7 diameter. This small range explains why disparity between the three results is magnified in the in-line direction. However, there is small discrepancy between them. Yang *et al.* (2008) results are 3% downstream in terms of the center of the eight type trajectory compared to Blackburn *et al.* (2000) and present results. In the present computations, we have verified that results are converged in terms of time step and space discretization.

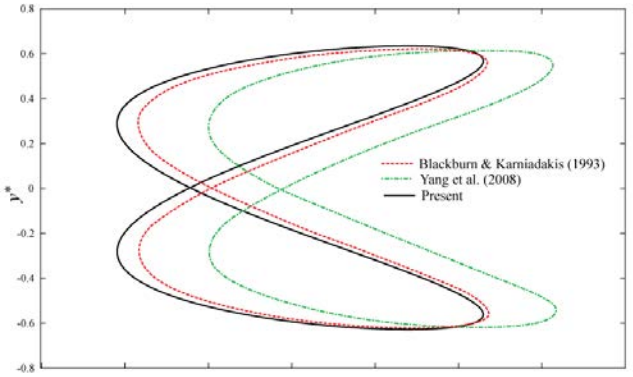

Figure 6: Trajectory of an isolated cylinder in cross-flow at U_r=5 and Re=200.

TANDEM ARRANGEMENT RESULTS

From now on, all results have been obtained with a mass ratio m^* of 1 and no structural damping considered. This means that damping comes from the flow only. Each cylinder obeys to equations of motion (2). The relation between the two definitions of the reduced velocities is from now on $U_r^* = \sqrt{2}U_r$. Note that the mesh deforms and follows the motion of cylinders. In the numerical procedure, boundaries stick to the cylinders at all times in an implicit manner since all the equations are solved simultaneously in a monolithic way. No remeshing process is performed which could be useful if cylinders were closer or for reduced velocities higher than 20. In these configurations, rigidities are so low that excursions of cylinders become very important and clashing between them may occur.

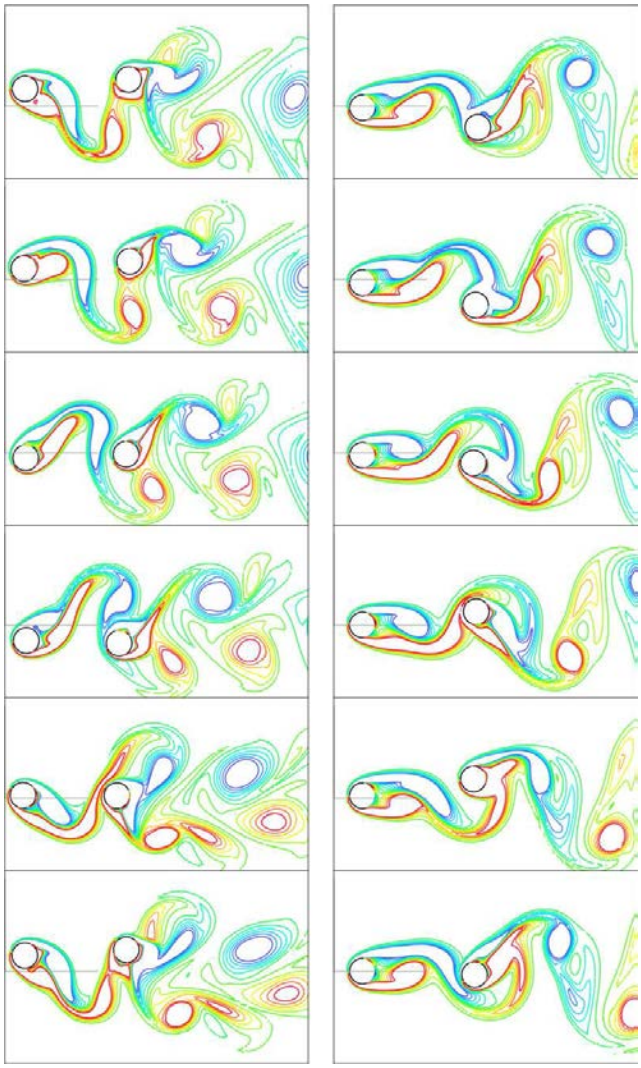

Figure 7 : Vorticity fields at nondimensional times 90, 91, 92, 93, 94, 95, 96. Left at U_r=6 and right at U_r=9.

Figure 7 shows vorticity fields in the tandem case at U_r = 6 and U_r= 9. The flow and cylinders behaviours are radically different. For U_r= 6, the first cylinder vibrates with an amplitude of 0.7D while the rear cylinder obeys to a non periodic behavior with amplitudes in the range 0.7 to 1.3D. For U_r = 9, the front cylinder experiences amplitudes of 0.2D while the rear one undergoes a periodical vibration of 1.1D amplitude. In all flow figures presented here red colour corresponds to positive values of the non-dimensioned vorticity ($\omega^* = \omega D/U$) while blue colour corresponds to negative values of the vorticity. Lower and upper bounds of the non-dimensioned vorticity isolines are -2 and 2.

Relative displacements of cylinders with respect to their initial positions are plotted on Figure 8 andFigure 9 for U_r = 6 and 9 respectively. One can easily observe that the downstream cylinder experiences much larger vibrations than the upstream one. Another observation is that when the front cylinder amplitude is large (see. U_r = 6), the deflection of the rear cylinder is smaller as experimentally observed by Germain *et al.* (2006). This can be viewed as a shielding effect. This means that the rear cylinder behaviour is influenced not only by the presence of the upstream cylinder but also by its vibrations. That justifies modeling the vibrational behaviour of the front cylinder.

Figure 10 shows the root-mean square of the transverse amplitude as a function of the reduced velocity. The curve corresponding to the leading cylinder corresponds well to that of an isolated cylinder. Large amplitudes are for reduced velocities ranging from 4 to 8. The downstream cylinder experiences low amplitudes for the small reduced velocities due to a shielding effect while larger amplitudes are obtained for Ur > 6. Also, one can observe that it experiences large vibrations even for reduced velocities as high as 16. This constitutes an important feature of the wake induced oscillations. Also, vibration amplitudes are lower than in Germain *et al.* (2006) since there is an important difference in the Reynolds number values with the present numerical results. In Germain *et al.* (2006) experiments, the Reynolds number ranges from 5500 to 50000. We know from Jauvtis and Williamson (2004) that a super-upper VIV phenomenon occurs for isolated vibrating two-degrees of freedom cylinders for Reynolds number values higher than 1000 and low mass ratios (m^*<3).

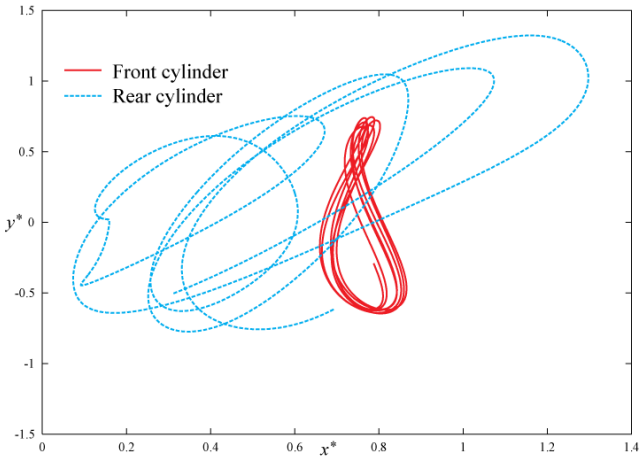

Figure 8 : Displacements of cylinders for the tandem case at U_r=6.

At the low Reynolds number value of 200 this phenomenon does not occur. One may infer that this will have an effect for arrays of cylinders. To reach higher values of the Reynolds number, Direct Numerical Simulations, *i.e.* three-dimensional computations without turbulence models, are required. This is beyond the scope of the present study. We evaluate in the context of our monolithic formulation that it would necessitate 500Go of RAM to perform such computations at Reynolds number value of 1000. We presently not have access to such computation facilities. Another difference with Germain *et al.* (2006)

experiments that may have an effect is that a pivoting system was used for which two-dimensionality of the cylinder motion is not fully ensured.

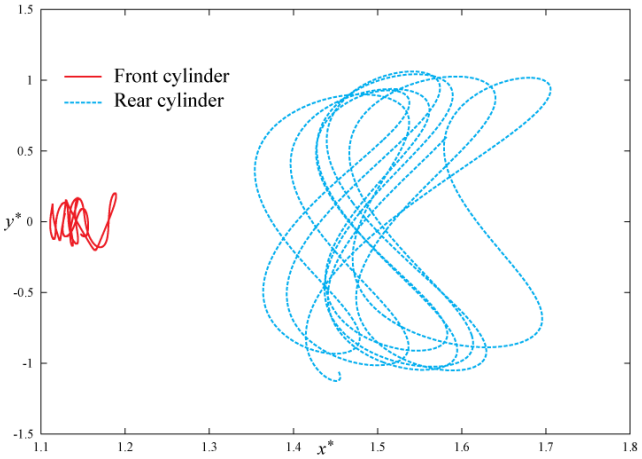

Figure 9 : Displacements of cylinders for the tandem case, U_r=9.

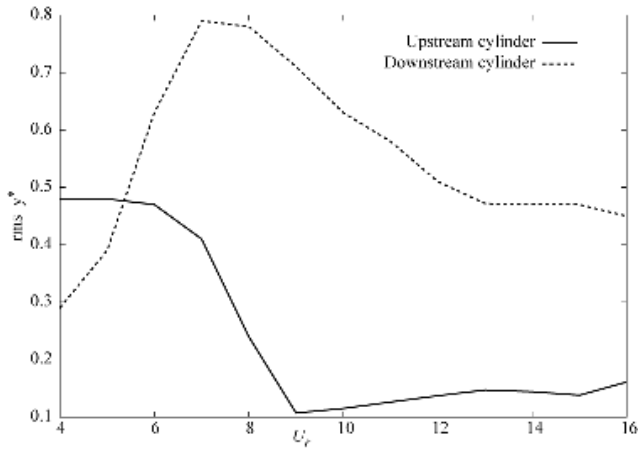

Figure 10 : Transverse displacements of cylinders in the tandem case for *Ur* ranging from 4 to 16.

THREE IN-LINE CYLINDERS ARRANGEMENT RESULTS

For the three in-line two-degree of freedom cylinders in cross-flow we present results for reduced velocities between 8 and 11.

It is interesting to compare trajectories of cylinders at the same reduced velocity between the tandem and three in-line cylinders cases. Such a comparison can be made at U_r = 9 between Figure 9 and Figure 12. At first sight, we observe similar trajectories for the two upstream cylinders, which was expected. However if we take a more precise look at the trajectory of the second cylinder, we can observe that it undergoes a smaller deflection in the flow direction for the 3 in-line array compared to the tandem case. This is due to a smaller drag resulting from the presence of the third cylinder in its wake. For the third cylinder, the trajectory is far from the 8-shape trajectory that is representative of VIV. Large excursions in *x* and *y* directions mean that the third cylinder experiences wake dynamics effects very different from those experienced by the second one.

The very perturbed cylinder trajectory of the third cylinder at U_r = 9 is not an isolated case. Indeed, taking a look at Figure 11 to Figure 14 clearly shows that the third cylinder experiences very distinguishable trajectories from the two upstream ones. Upstream cylinders observe classical eight shape trajectories while the third cylinder does not seem to follow a well defined or periodical trajectory.

From Figure 15, one can observe that the third cylinder is always located in vortical zones of the wake. This contributes largely to reducing its effective drag. The cylinder is also subject to stronger vortex effects on its sides at different times and may explain why its excursions are larger than the second cylinder.

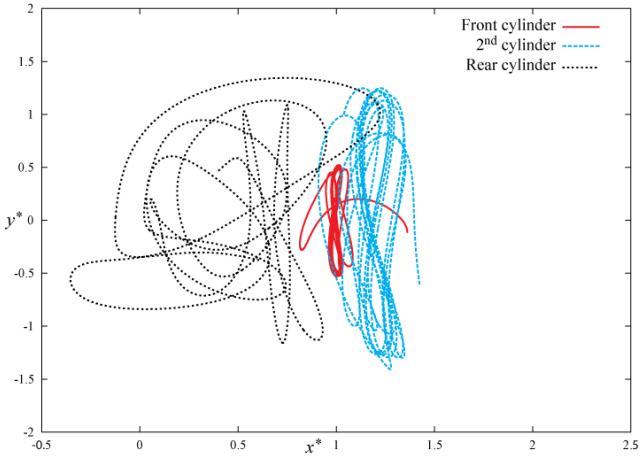

Figure 11 : Displacements of cylinders in the plane *x*-*y*, U_r = 8.

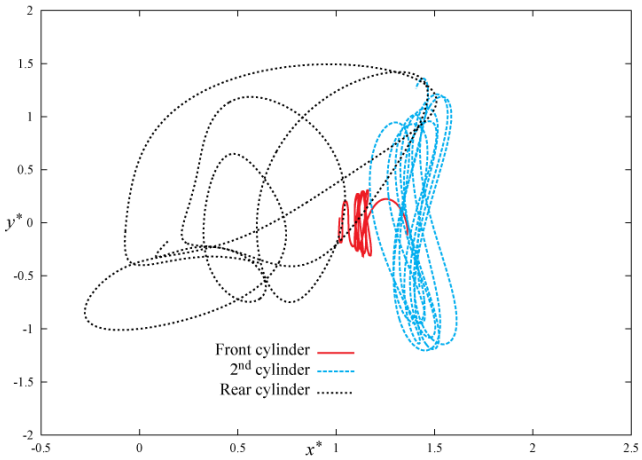

Figure 12 : Displacements of cylinders in the plane *x*-*y*, U_r = 9.

An important feature that one can notice from Figure 11 to Figure 14 is that the mean *x*-displacement of the third cylinder is half that of the two other cylinders. This is also observable on Figure 15. Whereas displacements in the flow direction of the upstream cylinders are comparable and depend on the reduced velocity, displacements of the third cylinder vary in the range -0.3 to 2 diameters which is of the same order of displacements variations in the *y*-direction. As an evidence, this greatly increases chances of clashing in the array. This has an effect on the computations. Indeed, the mesh cannot be squeezed to the limit where cylinders come into contact presently. Some remeshing process or ghost elements shall be introduced in the numerical

procedure to handle such situations. The present technique is able to handle gaps as low as 10% of a diameter. Nevertheless, for reduced velocities beyond 15 for the three cylinders arrays at L/D=4, there is contact. As this is not the point of the present study, we will keep that question for future work.

Finally, simulations should be performed on longer periods of time to extract frequency spectra of loads and displacements and eventually confirm these trends.

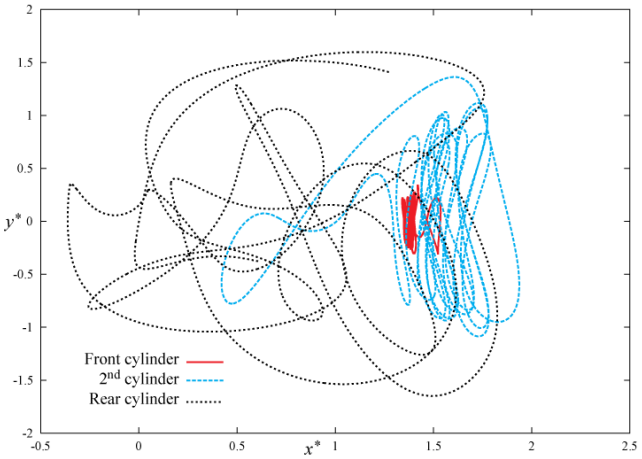

Figure 13 : Displacements of cylinders in the plane x-y, $U_r = 10$.

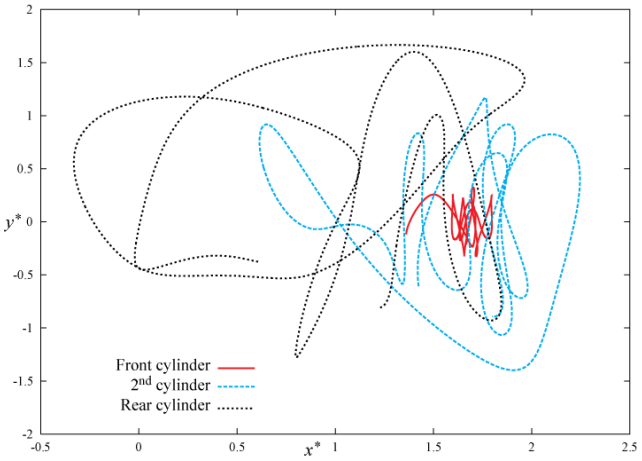

Figure 14 : Displacements of cylinders in the plane x-y, $U_r = 11$.

CONCLUSION

The flow around tandem and three in-line spring-supported cylinders arrays have been studied. Important specificities of such cases have been highlighted.

First, dynamics of upstream cylinders shall be modeled to fully take into account the wake dynamics. Indeed, these wake dynamics have a non negligible effect on downstream cylinders for low values of the reduced velocity or on the whole range for the three-cylinder cases.

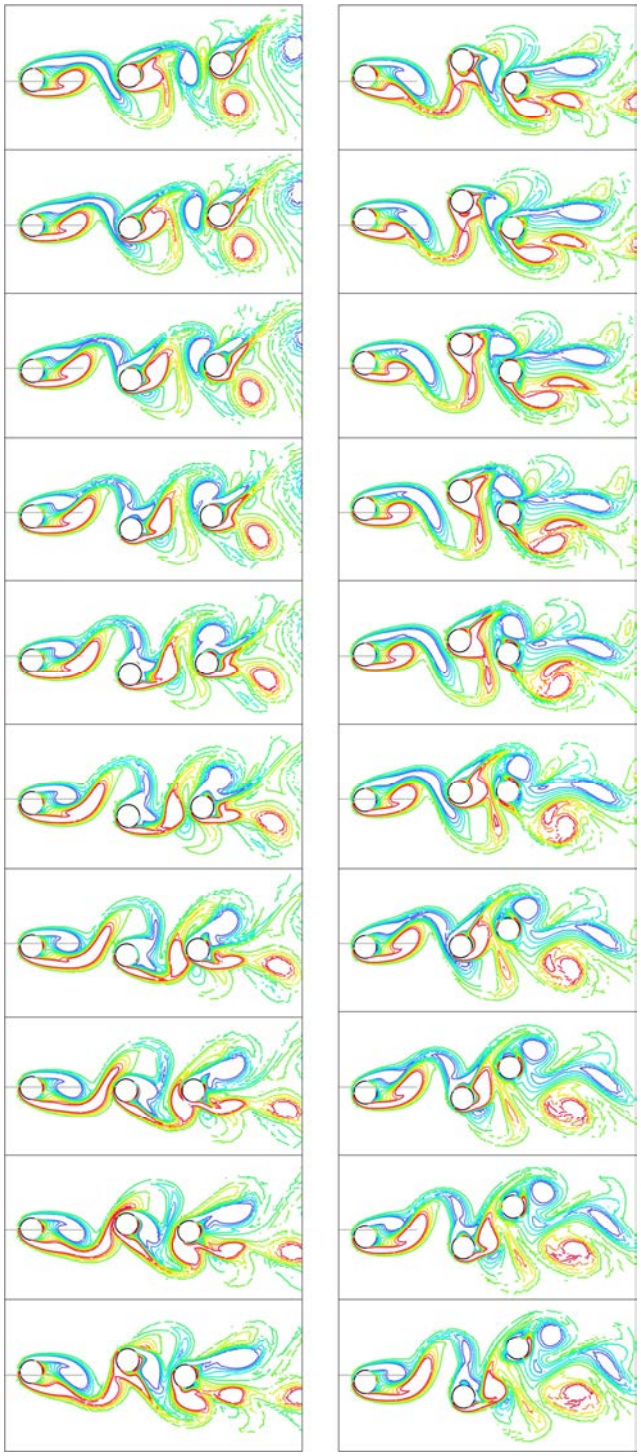
Figure 15 : Three-cylinder in-line array, Vorticity field at times 90 to 99.5 by increment of 0.5 from top to bottom and left to right, U_r =10.

For the tandem case and for a relatively large center-to-center spacing ratio, $L/D = 4$, the range over which vibrations of downstream cylinders occur is much broader than for an isolated cylinder, or the upstream cylinder. This corresponds to wake-induced oscillations (WIO) following the terminology by Germain *et al.* (2006). For smaller center-to-center spacings, these WIO may be emphasized since impacting flow dynamics are steeper. This will be the object of a separate study.

For the three in-line arrangement, the two upstream cylinders behave similarly to the two-cylinder case which was expected, but nevertheless experiencing lower drags due to the presence of the third cylinder, whereas the third cylinder experiences larger transverse and in-line excursions than both upstream cylinders.

For future work, the whole range of reduced velocities should be simulated to confirm observed trends. Larger time simulations should be performed to extract loads and displacements spectra. Finally, three-dimensional simulations are envisaged for more realistic comparisons with experimental data.

REFERENCES

Blackburn H, Govardhan R and Williamson C (2000). A complementary numerical and physical investigation of vortex-induced vibrations, *Journal of Fluids and Structures* **15**, 481–488.

Bokaian A and Geoola F (1984). Wake-Induced Galloping, *Journal of Fluid Mechanics* **146**, 383–415.

Braza M (1981). Etude numérique du décollement instationnaire externe par une formulation vitesse-pression : Application à l'écoulement autour d'un cylindre circulaire. *Thèse de docteur-ingénieur, Institut National Polytechnique, Toulouse*.

Chagnon M (2008). Étude d'un écoulement autour de deux cylindres placés en tandem. *Summer training report, École Polytechnique de Montréal.*

Etienne S (2008). Vortex Induced Vibrations and galloping of two cylinders placed in tandem arrangement, *in 18th Intl. Offshore and Polar Engng Conf. (ISOPE)*.

Etienne S, Garon A and Pelletier D (2009). Perspective on the Geometric Conservation Law and Finite Element Methods for ALE Simulations of Incompressible Flow, *Journal of Computational Physics* **228**, 2313-2333.

Fregonesi R, Saltara F, Meneghini J and Ferrari J (2001). Flow interference around two circular oscillating cylinders, *in Proc. OMAE2001*.

Germain G, Gaurier B, Boulluec M L, Fontaine E and Capul J (2006). Vortex and wake effects on closely spaced marine risers, *in Proc. PVP2006*.

Halse K H (1997). On vortex shedding and predictions of VIV of circular cylinders, *PhD Thesis, NTNU Trondheim*.

Huhe-Aode, Tatsuno M and Taneda S (1985) .Visual studies of wake structure behind two cylinders in tandem arrangement, reports of Research Institutes for Applied Mechanics, Fukuoka, Vol. XXXII, **99**, 1-20.

Jauvtis N, Williamson C H K (2004). The effect of two degrees of freedom om vortex-induced vibration at low mass and damping, *Journal of Fluid Mechanics*, **509**, 23-62.

Mittal S and Kumar V (2001). Flow-induced oscillations of two cylinders in tandem and staggered arrangement, *Journal of Fluids and Structures* **15**, 717–736.

Mittal S and Kumar V (2004). Vortex-induced vibrations of a pair of cylinders at Reynolds number 1000, *International Journal of Computational Fluid Dynamics* **18**, 601–614.

Okajima A (1979). Flows around two tandem circular cylinders at very high Reynolds number, *Bull. JSME* **22**, 504

Igarashi T: Trans. Jpn. Soc. Mech. Eng. B **46**, 1026 (1980).

Moriya M, Sakamoto H, Kiya M and Mikio A: Trans. Jpn. Soc. Mech. Eng. B **49**, 1364 (1983).

Potanza J, Chen C and Chen H (2005). Simulation of high Reynolds number flow past arrays of circular cylinders undergoing vortex-induced vibrations, *in Proc. 15th Intl. Offshore and Polar Engng Conf. (ISOPE)*.

Sa J Y and Chang KS (1991). Shedding patterns of the near wake vortices behing a cylinder, *International Journal for Numerical Methods in Fluid,* **12,** 463-474.

Schenk O and Gärtner K, (2004) Solving Unsymmetric Sparse Systems of Linear Equations with PARDISO, *Journal of Future Generation Computer Systems*, **20(3)** 475--487.

Schenk O and Gärtner K, (2006) On fast factorization pivoting methods for symmetric indefinite systems, *Elec. Trans. Numer. Anal.,* **23**, 158-179.

Yang J, Preidikman S and Balaras E (2008). A strongly coupled, embedded-boundary method for fluid-structure interactions of elastically mounted rigid-bodies, *Journal of Fluids and Structures* **24**, 167–182.

Zdravkovitch M (1977). Review of flow interference between two circular cylinders in various arrangements, Trans. ASME, 618-623.

Zdravkovitch M (1985). Flow induced oscillations of two interfering circular cylinders, *Journal of Sound and Vibrations* **101**, 511–521.